



Published in final edited form as:

*Oncogene*. 2012 August 9; 31(32): 3679–3695. doi:10.1038/onc.2011.545.

## ***Suppression of Tumorigenicity-14, encoding matriptase, is a critical suppressor of colitis and colitis-associated colon carcinogenesis***

**Peter Kosa, Roman Szabo, Alfredo A. Molinolo, and Thomas H. Bugge**

Oral and Pharyngeal Cancer Branch, National Institute of Dental and Craniofacial Research, National Institutes of Health, Bethesda, MD 20892

### **Abstract**

Colitis-associated colorectal cancers are an etiologically distinct subgroup of colon cancers that occur in individuals suffering from inflammatory bowel disease and arise as a consequence of persistent exposure of hyperproliferative epithelial stem cells to an inflammatory microenvironment. An intrinsic defect in the intestinal epithelial barrier has been proposed to be one of several factors that contribute to the inappropriate immune response to the commensal microbiota that underlies inflammatory bowel disease. Matriptase is a membrane-anchored serine protease encoded by *Suppression of Tumorigenicity-14 (ST14)* that strengthens the intestinal epithelial barrier by promoting tight junction formation. Here we show that intestinal epithelial-specific ablation of *St14* in mice causes formation of colon adenocarcinoma with very early onset and high penetrance. Neoplastic progression is preceded by a chronic inflammation of the colon that resembles human inflammatory bowel disease and is promoted by the commensal microbiota. This study demonstrates that inflammation-associated colon carcinogenesis can be initiated and promoted solely by an intrinsic intestinal permeability barrier perturbation, establishes *St14* as a critical tumor suppressor gene in the mouse gastrointestinal tract, and adds matriptase to the expanding list of pericellular proteases with tumor suppressive functions.

### **Introduction**

Colitis-associated colorectal cancers are etiologically and molecularly distinct from familial adenomatous polyposis coli-associated colorectal cancer, hereditary non-polyposis coli colorectal cancer, and sporadic colorectal cancer. The malignancy occurs in individuals suffering from ulcerative colitis or Crohn's disease (collectively, inflammatory bowel disease) with an incidence that is proportional to duration of the disease. The neoplastic progression of disease-stricken colonic epithelium is believed to be driven by the chronic inflammatory microenvironment, which promotes the progressive genomic instability of

Users may view, print, copy, download and text and data- mine the content in such documents, for the purposes of academic research, subject always to the full Conditions of use: [http://www.nature.com/authors/editorial\\_policies/license.html#terms](http://www.nature.com/authors/editorial_policies/license.html#terms)

Address correspondence and reprint requests to: Thomas H. Bugge, Ph.D., Proteases and Tissue Remodeling Section, Oral and Pharyngeal Cancer Branch, National Institute of Dental and Craniofacial Research, National Institutes of Health, 30 Convent Drive, Room 211, Bethesda, MD 20892, Phone: (301) 435-1840, Fax: (301) 402-0823, [thomas.bugge@nih.gov](mailto:thomas.bugge@nih.gov).

#### **Conflict of interest**

The authors declare no competing financial interests in relation to the work described.

colonic epithelial stem cells by inducing sustained hyperproliferation (regenerative atypia) and by the continuous presence of high local concentrations of DNA damaging agents, such as reactive oxygen species (reviewed in (Danese and Mantovani, 2010, Saleh and Trinchieri, 2011)).

While there is considerable debate about the relative importance of the specific factors that contribute to the development of inflammatory bowel disease, there is a consensus that the disease represents an inappropriate immune response to the commensal microbiota in genetically predisposed individuals (reviewed in (Kaser *et al.*, 2010, Saleh and Trinchieri, 2011, Schreiber *et al.*, 2005, Van Limbergen *et al.*, 2009, Xavier and Podolsky, 2007)). In this regard, the contribution of aberrant inflammatory circuits to the development of inflammatory bowel disease has been clearly established by genetic analysis, including genome-wide association studies, that have linked loss of function mutations or polymorphisms in genes encoding interleukins, interleukin receptors, chemokine receptors, nucleotide-binding oligomerization domain (NOD)-like receptors, toll-like receptor 4, intelectins, and prostaglandin receptors to ulcerative colitis, to Crohn's disease or to both. Further support for a principal role of derailed inflammatory circuits is gained from the spontaneous inflammatory bowel disease observed in mice deficient in a variety of immune effectors (reviewed in (Kaser *et al.*, 2010, Saleh and Trinchieri, 2011, Schreiber *et al.*, 2005, Van Limbergen *et al.*, 2009, Xavier and Podolsky, 2007)). Much less explored is the importance of individual components of the intestinal epithelial barrier in preventing inflammatory bowel disease, and the potential contribution of intrinsic intestinal epithelial barrier defects to the development of the syndrome. The clearest indication of the potential importance of primary barrier integrity comes from studies of mice with germline ablation of *Muc2* encoding the major mucin that shields the intestinal epithelium from direct contact with the microbiota. These mice develop colitis, which may progress to colon adenocarcinomas in older animals (Velcich *et al.*, 2002). Additional evidence has been obtained from transgenic mice with intestinal epithelial-specific overexpression of myosin light chain kinase, which display decreased barrier function and increased immune activation, although an inflammatory bowel-like syndrome did not emerge in the absence of additional immunological challenges (Su *et al.*, 2009).

Matriptase is a member of the recently established family of type II transmembrane serine proteases that is encoded by the *Suppression of Tumorigenicity-14 (ST14)* gene (Bugge *et al.*, 2009, Kim *et al.*, 1999, Lin *et al.*, 1999, Takeuchi *et al.*, 1999, Tanimoto *et al.*, 2001). *ST14* was originally proposed to be a colon cancer tumor suppressor gene, due to its specific down-regulation in adenocarcinomas of the colon (Zhang *et al.*, 1998). Matriptase is expressed in multiple epithelia of the integumental, gastrointestinal, and urogenital systems, where it has pleiotropic functions in the differentiation or homeostasis of both simple and stratified epithelia, at least in part through the proteolytic activation of the epithelial sodium channel activator, prostasin/PRSS8 (Szabo and Bugge, 2011). In simple epithelium of the gastrointestinal tract, a principal function of matriptase is to promote the formation of a paracellular permeability barrier, possibly through the posttranslational regulation of the composition of claudins that are incorporated into the epithelial tight junction complex of differentiating intestinal epithelial cells (Buzza *et al.*, 2010, List *et al.*, 2009).

Through lineage-specific loss of function analysis in mice we now have examined the role of *St14* as a tumor suppressor gene. Interestingly, we found that the selective ablation of *St14* from intestinal epithelium results in the formation of adenocarcinoma of the colon with very early onset and high penetrance. Neoplastic progression occurs in the absence of exposure of animals to carcinogens or tumor promoting agents, is preceded by chronic colonic inflammation that resembles human inflammatory bowel disease, and can be suppressed by aggressive antibiotics treatment. The study demonstrates that inflammation-associated colon carcinogenesis can be initiated solely by intrinsic paracellular permeability barrier perturbations, and establishes that *St14* is a critical tumor suppressor gene in the mouse gastrointestinal tract.

## Results

### Meta-analysis of transcriptomes shows decreased expression of ST14 in human colon adenomas and adenocarcinomas

We first performed *in silico* data mining of the Oncomine microarray database (Rhodes *et al.*, 2004) to corroborate the initial report of reduced *ST14* expression in human colon cancer (Zhang *et al.*, 1998) (Figure 1). Interestingly, *ST14* was significantly downregulated compared to normal colon in seven of the fourteen published studies listed in the database (studies A and C–H), whereas six studies showed no change (studies B and J–N) and a single study (study I) found *ST14* to be upregulated (Figure 1 and Supplementary Table 1). Of the fourteen studies, study A, which compared gene expression in colorectal dysplastic adenomatous polyps to normal colonic epithelium, was conducted using laser capture microdissected tissue (*ST14* downregulation,  $P < 0.0006$ ) (Gaspar *et al.*, 2008), and therefore provided the most reliable estimate of *ST14* expression in normal and dysplastic colonic epithelium.

### St14-ablated colonic epithelium undergoes rapid and spontaneous malignant transformation

To specifically explore the functional consequences of intestinal loss of *St14* on colon carcinogenesis, we interbred mice carrying an *St14<sup>LoxP</sup>* allele (List *et al.*, 2009) with mice carrying an *St14* null allele (*St14<sup>-</sup>*) and mice carrying a *Cre* transgene under the control of the intestinal-specific villin promoter (*villin-Cre<sup>+</sup>*) (Madison *et al.*, 2002). This resulted in the generation of *villin-Cre<sup>+/0</sup>;St14<sup>LoxP/-</sup>* mice (hereafter termed *St14<sup>-</sup>* mice) and their associated littermates *villin-Cre<sup>+/0</sup>;St14<sup>LoxP/+</sup>*, *villin-Cre<sup>0</sup>;St14<sup>LoxP/-</sup>*, and *villin-Cre<sup>0</sup>;St14<sup>LoxP/+</sup>* (hereafter termed *St14<sup>+</sup>* mice). As reported recently (List *et al.*, 2009), this strategy resulted in the efficient deletion of matriptase from the entire intestinal tract, as shown by the loss of matriptase immunoreactivity in colon (compare Supplementary Figure 1a and b) and small intestine (compare Supplementary Figure 1c and d), and by highly diminished *St14* transcript abundance (Supplementary Figure 1e). *St14<sup>-</sup>* mice were outwardly unremarkable at birth, but displayed significant growth retardation after weaning (Supplementary Figure 1f). Examination of prospective cohorts of *St14<sup>-</sup>* mice and their associated littermate controls revealed that intestinal *St14* ablation greatly diminished life span (Supplementary Figure 1g).

Unexpectedly, histological analysis of moribund *St14*<sup>-</sup> mice revealed the presence of invasive adenocarcinoma of the colon in 8 of 24 (33%) of *St14*<sup>-</sup> mice examined at four to 18 weeks of age (Table 1, Figure 2a, b, and d) and dysplastic colonic epithelium (regenerative atypia) in the remaining 16 mice (Table 1 and Figure 2d). Remarkably, in light of the fact that these mice were not carcinogen treated or exposed to other insults to the intestinal tract, adenocarcinoma could be found in mice less than five weeks of age (Table 1). All adenocarcinomas had progressed to invade the muscularis mucosae underlying the colonic epithelium and the subadjacent muscularis externa (Figure 2a and b). Furthermore, in six of eight (75%) adenocarcinomas examined, the tumor cells had infiltrated the lymphatic vasculature, as revealed by combined immunohistochemical staining with pan-keratin antibodies and antibodies against the lymphatic endothelial marker, LYVE-1 (Table 1 and Figure 2c and d). The tumors displayed many hallmarks of human colitis-associated colon cancer, including activation of  $\beta$ -catenin (Figure 3a and a'), dysorganized basement membrane deposition (Figure 3b and b'), fibrosis (Figure 3c and c'), severe dysplasia with abundant atypical mitosis (Figure 3d), epithelial hyperproliferation (Figure 4a and a'), loss of terminal differentiation (Figure 4b and b'), and chronic inflammatory cell infiltrates (Figure 4c and c', d and d'). Importantly, the small intestine was histologically unremarkable in all mice examined (data not shown), although *St14* was efficiently ablated also from this tissue (Supplementary Figure 1d and e). Taken together, these data show that *St14* is a critical tissue-specific tumor suppressor gene in the mouse intestine that suppresses the formation of early, invasive adenocarcinomas of the colon.

### Impaired barrier function in *St14*-ablated colon

We have previously shown that either reduced matriptase expression or global postnatal ablation of matriptase from all tissues results in impaired intestinal barrier function (Buzza *et al.*, 2010, List *et al.*, 2009), suggesting that this would also be a feature of mice with intestinal epithelial-specific embryonic deletion of matriptase. To examine colonic and small intestinal barrier function, we injected a reactive biotin tracer into the intestinal lumen of three week old *St14*<sup>-</sup> and littermate *St14*<sup>+</sup> mice and followed the fate of the marker using fluorescent streptavidin. Compatible with an intact intestinal barrier function, the biotin marker decorated the surface of colonic crypts and villi of the small intestine, but did not penetrate into the tissue of *St14*<sup>+</sup> mice (Figure 5a and d). In contrast, just three minutes after intraluminal biotin injection, the biotin tracer could be found on the basolateral membranes and on connective tissue cells of the colon and small intestine of *St14*<sup>-</sup> mice demonstrating a profound failure to establish a functional intestinal barrier (Figure 5b and e).

### Neoplastic progression occurs within a chronic inflammatory colonic microenvironment that resembles inflammatory bowel disease

*St14*-ablated colonic tissue was histologically unremarkable when examined at birth and at postnatal day five (compare Figures 6a and a', b and b'). The first observable pathological manifestation (day 10) was the detachment and apoptosis (anoikis) of distal crypt cells (compare Figure 6c and c'). This was followed by the failure of colonic epithelial cells to undergo proper terminal differentiation, as evidenced by cessation of mucin formation (data not shown). Thereafter, *St14*<sup>-</sup> colons entered a progressively hyperplastic inflammatory and ulcerative state that eventually resulted in the gross distortion of colonic tissue architecture

(compare Figure 6d and d', and 6e and e'). BrdU incorporating cells initially were confined to the bottom of the crypts, but later were present also in distal segments of the crypts (data not shown). Inflammatory infiltrates were evident at day 15. Inflammation at first was mild, but rapidly became severe, with inflammatory cells eventually constituting the dominant cell population of the mucosa and submucosa. Polyps were not observed in any of the examined colons prior to malignant transformation, indicating that *St14* ablation-associated adenocarcinomas, like inflammatory bowel disease-associated colorectal cancers arise from flat lesions within hyperproliferative and inflamed mucosa.

### **Abnormal epithelial differentiation and activation of inflammatory pathways precede inflammatory bowel disease-like colitis and dysregulation of common colon cancer-associated signaling pathways**

To elucidate the molecular events that precede the early development of colitis in mice with matriptase-ablated colonic epithelium, we next performed stage-specific transcriptomic analysis using whole-genome arrays. We selected two time points (days 0 and 5) where matriptase-ablated colonic epithelium was histologically normal, and one time point (day 10) where pathological changes were emerging (see above). The analysis was repeated four times for each of the three time points by analyzing individual *St14*<sup>-</sup> mice and their associated *St14*<sup>+</sup> littermates. Genes that were more than two-fold up or downregulated in each of the four separate experiments were considered for analysis. No significant differences in the transcriptomes of *St14*-ablated and *St14*-sufficient colons were apparent at day 0 (data not shown). Interestingly, however, dysregulation of epithelial differentiation was apparent already at day 5 and was pronounced at day 10 (Tables 2 and 3). This was evidenced by the conspicuous upregulation of genes typically expressed in basal, suprabasal or keratinizing layers of stratified squamous epithelium lining the oral cavity, interfollicular epidermis, hair and nails of follicular epidermis, and filiform papillae of the tongue. These included keratin 14 (*Krt14*), keratin 36 (*Krt36*), keratin 84 (*Krt84*), small protein-rich protein 1a (*Sprr1a*), small protein-rich protein 2h (*Sprr2h*), and secreted Ly6/Plaur domain containing 1 (*Slurp1*). Abnormal colonic epithelial differentiation at day five was further evidenced by the downregulation of the expression of Paneth cell-specific alpha-defensin 4 (*Defa4*). Although *St14*<sup>-</sup> colonic tissues were histologically normal at day 5, activation of inflammatory pathways was evidenced by the increased expression of several inflammation-associated genes, including chemokine (C-X-C motif) ligand-1 (*Cxcl1*), matrix metalloproteinase 10 (*Mmp10*), lymphocyte antigen 6 complex, locus C2 (*Ly6c2*), tumor necrosis factor (*Tnf*), myelin and lymphocyte protein (*Mal*), serum amyloid A3 (*Saa3*), lymphocyte antigen 6 complex, locus I (*Ly6i*), lymphocyte antigen 6 complex, locus D (*Ly6d*), and GPI-anchored molecule-like protein (*Gml*). Inflammatory circuit activation was manifest at day 10, with upregulated expression of a number of additional inflammation-associated genes, including receptor-interacting serine-threonine kinase 3 (*Ripk3*), lipopolysaccharide binding protein (*Lbp*), lactotransferrin (*Ltf*), TNFAIP3 interacting protein 3 (*Tnip3*), secretory leukocyte peptidase inhibitor (*Slpi*), leucine-rich alpha-2-glycoprotein 1 (*Lrg1*), and chemokine (C-X-C motif) ligand 5 (*Cxcl5*). Several epithelial proliferation-associated genes also were upregulated at day 10, including genes encoding the growth factors amphiregulin (*Arege*), heparin binding EGF-like growth factor (*Hbegf*), and the p53-binding proliferation inducer, tripartite-motif containing-29 (*Trim29*). Taken together, the

combined stage-specific histological and transcriptomic analysis show that colonic epithelial ablation of matriptase causes aberrant early postnatal epithelial differentiation that triggers expression of pro-inflammatory mediators, which in turn causes persistent inflammation and chronic epithelial hyperproliferation.

Colonic tumor initiation in humans and animal models frequently is linked to dysregulated BMP, Notch, and Wnt signaling, leading to the expansion of the colonic stem cell population (de Lau *et al.*, 2007, Hardwick *et al.*, 2008, Medema and Vermeulen, 2011, Zeki *et al.*, 2011). We therefore examined the level of expression of several putative and validated colonic stem cell markers (*Aldh1a1*, *Ascl2*, *Ets2*, *Lgr5*, *Phlda1*), as well as BMP (*Cbfb*, *Dlx2*, *Hes1*, *Id1*, *Id2*, *Id3*, *Id4*, *Junb*, *Sox4*, *Stat1*), Notch (*Cdkn1a*, *Ccdn1*, *Cdk2*, *Hes1*, *Hes6*, *Klf4*, *Myc*, *Nfkb2*), and Wnt (*Ascl2*, *Axin2*, *Cd44*, *Csnk1a1*, *Csnk1d*, *Csnk1e*, *Cttnb1*, *Cryll1*, *Ephb2*, *Ephb3*, *Gfi1*, *Hdac2*, *Id3*, *Ihh*, *Lef1*, *Myc*, *Nkd1*, *Nlk*, *Pascin2*, *Pcna*, *Plat*, *Rbbp4*, *Snai1*, *Sox4*, *Sox9*, *Spdef*, *Stra6*, *Tcf4*, *Yes1*) target genes in *St14*<sup>-</sup> mice and their associated *St14*<sup>+</sup> littermates (Supplementary Table 2). This transcriptomic analysis provided no clear evidence of stem cell expansion or dysregulation of either of the three signaling pathways at day 0, at day 5, when abnormal differentiation and innate immune activation were apparent, or even at day 10, when abnormal colonic morphology was manifest. In agreement with this analysis, expression of the Wnt target, *Sox9*, in *St14*<sup>-</sup> mice was appropriately confined to the crypts at day 10, and aberrant localization of *Sox9* was not detected until day 15 (Supplementary Figure 2).

### Diminution of the intestinal microbiota retards development of inflammatory bowel disease-like colitis

We hypothesized that the chronic inflammatory microenvironment that facilitated neoplastic progression of *St14*-ablated colonic epithelium was generated in part by increased exposure of the mucosal immune system to the resident microbiota due to impaired barrier formation and aberrant differentiation. To challenge this hypothesis, we next treated weaning-age *St14*<sup>-</sup> mice with a cocktail of the four antibiotics, ampicillin, neomycin, metronidazole, and vancomycin or with vehicle for two weeks, a standard procedure for cleansing of the intestinal microbiota (Rakoff-Nahoum *et al.*, 2004). Due to the failure of some of the four antibiotics to be present in milk, the treatment was initiated at weaning, when significant pre-neoplastic progression was already apparent (Figure 6e and e'). As expected, antibiotics treatment reduced the colonic bacterial load by approximately 1,500-fold, as judged by the abundance of bacterial 16S ribosomal DNA in feces (Figure 7a), without compromising body weight (Figure 7b). *Helicobacter* is found commonly in the commensal microbiota of mice and promotes neoplastic progression in a variety of models of colon carcinogenesis (Engle *et al.*, 2002, Erdman *et al.*, 2003, Hale *et al.*, 2007, Maggio-Price *et al.*, 2006, Newman *et al.*, 2001). We therefore specifically determined the presence of *Helicobacter* DNA in feces of antibiotics-treated and untreated *St14*<sup>-</sup> mice by PCR analysis (Supplementary Table 3). Nine of 17 (53%), 7/17 (41%), and 1/17 (6%) of control mice tested were positive for *Helicobacter typhlonius*, *Helicobacter rodentium*, and an undetermined *Helicobacter* species, respectively, whereas 2/13 (15%) of the analyzed antibiotics-treated mice were positive for *Helicobacter typhlonius*. Although initiated only after weaning, antibiotics treatment markedly blunted abnormal epithelial differentiation,

epithelial hyperproliferation and inflammation of the colon. This was evidenced by a quantitative reduction in colonic mucosal thickness (Figure 7c), increased mucin production (Figure 7d, Figure 8a and b), decreased epithelial proliferation (Figure 7e, Figure 8c and d), and decreased inflammatory cell infiltration (Figure 7f–h, Figure 8e–j), although the diminution of T-cell and neutrophil abundance did not reach statistical significance. Furthermore,  $\beta$ -catenin expression levels were normalized in two of four antibiotics-treated *St14*<sup>-</sup> mice when analyzed by immunoblot (Supplementary Figure 3A, compare lanes 7–10 with 13 and 14), and Sox9 was only infrequently found in the distal portion of the colonic crypts of antibiotics-treated *St14*<sup>-</sup> mice (Supplementary Figure 2d and e), suggesting a diminution of Wnt signaling. Analysis of BMP (phospho-SMAD1/5) and Notch1 (Notch1 intracellular domain) signaling did not reveal a treatment- or genotype-specific pattern, but the abundance of each of the two protein species in intestinal tissue extracts was difficult to assess accurately (Supplementary Figure 3B).

Taken together, the data are compatible with a principal role of the commensal microbiota in pre-neoplastic progression. A mechanistic model for matriptase ablation-induced colon cancer based on the above findings is shown in Figure 9. We propose that the intrinsic defect in barrier function associated with the failure to form functional tight junctions (Buzza *et al.*, 2010, List *et al.*, 2009) causes increased exposure of the immune system to the commensal microbiota. This exposure elicits vigorous inflammatory and repair responses that involve epithelial stem cell activation and are continuous, rather than transient, due to the inherent failure of matriptase-ablated colonic epithelial cells to establish a functional barrier. The sustained hyperproliferation of epithelial stem cells within a genotoxic chronic inflammatory microenvironment in turn induces the progressive genomic instability and subsequent rapid malignant conversion.

## Discussion

It has long been suspected that intrinsic alterations in the paracellular intestinal permeability barrier in humans could be a priming factor for the development of the aberrant immune response to the commensal microbiota that underlies inflammatory bowel disease and its associated malignancies. The current study now provides strong experimental support for this notion by showing that intestinal epithelial-specific ablation of matriptase - a membrane-anchored serine protease that is essential for intestinal epithelial tight junction formation - causes a commensal microbiota-dependent inflammatory bowel disease-like colitis that very rapidly progresses to adenocarcinoma. The spontaneous and rapid malignant transformation of the colonic epithelium furthermore demonstrates that a simple increase in intestinal paracellular permeability suffices to both initiate and drive inflammation-associated adenocarcinoma formation. This finding parallels the recent identification of the permeability of the epidermal barrier as a major determinant of the development of other chronic inflammatory diseases, including ichthyosis vulgaris, atopic eczema, and asthma (Sandilands *et al.*, 2009, Smith *et al.*, 2006). Previously published animal models of inflammatory bowel disease-associated colorectal cancer include dextran sodium sulphate- or dextran sodium sulphate combined with azoxymethane-induced chemical colon carcinogenesis in inbred mouse strains (Okayasu *et al.*, 1996, Okayasu *et al.*, 2002), and genetic models, including germline *Il10*- (Berg *et al.*, 1996), combined germline *Tbx21*- and

*Rag2*- (Garrett *et al.*, 2009), myeloid lineage *Stat3*- (Deng *et al.*, 2010), myeloid lineage *Itgav*- (Lacy-Hulbert *et al.*, 2007), germline *Gnai2*- (Rudolph *et al.*, 1995), and combined germline *Il2*- and *b2m*-ablated mice (Shah *et al.*, 1998). In these models, colitis and colon carcinoma occur as a consequence of either a sustained chemical damage to the colonic epithelium or perturbation of the immune system through elimination of key effectors of innate or adaptive immunity. Compared to the above models, colon carcinogenesis in intestinal *St14*-ablated mice appears to display some unique features. First, it is initiated by a loss of intestinal barrier function, which is associated with aberrant differentiation and immune activation, but these priming events initially occur in the absence of detectable perturbation of common colon cancer-associated signaling pathways (Kaiser *et al.*, 2007). Second, adenocarcinoma with involvement of lymphoid tissues is observed even in very young animals. This very rapid neoplastic progression may be explained, at least in part, by the presence of various helicobacter species in the intestinal microbiota of *St14*<sup>-</sup> mice, as colon carcinogenesis in several mouse models has been shown to be accelerated by or to be dependent upon helicobacter colonization (Engle *et al.*, 2002, Erdman *et al.*, 2003, Hale *et al.*, 2007, Maggio-Price *et al.*, 2006, Newman *et al.*, 2001).

In light of the findings in this study, it is tempting to speculate that neoplastic progression in previously described mouse models of inflammatory bowel disease-associated colorectal cancer (and perhaps colitis-associated human colorectal cancer) may be accelerated by an immune activation-induced decrease in the intestinal paracellular permeability barrier caused by downregulating the activity of matriptase or other molecules within a matriptase-dependent proteolytic pathway that facilitates tight junction formation.

Conclusive links have been forged between increased activity of multiple members of the complement of extracellular and pericellular proteases and the initiation and progression of a wide variety of human malignancies (reviewed in (Andreasen *et al.*, 2000, Borgono and Diamandis, 2004, Kessenbrock *et al.*, 2010, Mohamed and Sloane, 2006, Netzel-Arnett *et al.*, 2003)). Much less studied is the capacity of extracellular/pericellular proteases to act as suppressors of tumorigenesis (reviewed in (Lopez-Otin and Matrisian, 2007, Lopez-Otin *et al.*, 2009)). Induced germline or lineage-specific gene deletion studies in mice as well as spontaneous somatic mutation analysis of human cancers have provided direct evidence for a tumor suppressive function of MMP3 (McCawley *et al.*, 2004, McCawley *et al.*, 2008), MMP8 (Balbin *et al.*, 2003, Palavalli *et al.*, 2009), MMP12 (Acuff *et al.*, 2006), and Cathepsin L (Reinheckel *et al.*, 2005). Furthermore, the frequent epigenetic and genetic silencing of other extracellular and pericellular proteases in human cancers and the ability to inhibit distinct steps of tumor progression in experimental models of cancer through modulation of their level of expression suggest that the number of extracellular and pericellular proteases with tumor suppressive function may be substantial (reviewed in (Lopez-Otin and Matrisian, 2007, Lopez-Otin *et al.*, 2009)). The current study adds matriptase to the above list of pericellular proteases with tumor suppressive functions. Matriptase, however, so far is unique among pericellular proteases in the sense that its absence by itself suffices to cause malignancy, whereas tumor suppressive function of other proteases was revealed in chemical and transplantation models of cancer.

Previous studies have shown that overexpression of matriptase can initiate carcinogenesis and accelerate the dissemination of a variety of carcinomas in diverse model systems. This property of matriptase is owed at least in part to its ability to autoactivate (Oberst *et al.*, 2003) and subsequently serve as an initiator of several intracellular signaling and proteolytic cascades through proteolytic maturation of growth factors, protease activated receptor activation, and protease zymogen conversion (Bhatt *et al.*, 2007, Cheng *et al.*, 2009, Forbs *et al.*, 2005, Ihara *et al.*, 2002, Jin *et al.*, 2006, Kilpatrick *et al.*, 2006, Lee *et al.*, 2000, List *et al.*, 2005, Netzel-Arnett *et al.*, 2006, Owen *et al.*, 2010, Sales *et al.*, 2010, Suzuki *et al.*, 2004, Szabo *et al.*, 2011, Takeuchi *et al.*, 2000, Ustach *et al.*, 2010). The dual ability of a protease to promote carcinogenesis in some contexts, while suppressing carcinogenesis in others, is rare, but not entirely unprecedented. A clear example is given by the tumor promoting effect of transgenic misexpression of the stromal protease, MMP3, in the mammary epithelial compartment, as opposed to the strong protection of mice from chemically-induced squamous cell carcinogenesis caused by germ-line ablation of the protease (McCawley *et al.*, 2004, McCawley *et al.*, 2008, Sternlicht *et al.*, 1999, Sternlicht *et al.*, 2000). Additional proteases, such as MMP9, MMP11, and MMP19 may also promote or suppress, respectively, malignant progression in a stage or tissue-dependent manner (Lopez-Otin and Matrisian, 2007).

In conclusion, our study has uncovered a critical role of the transmembrane serine protease matriptase in preserving immune homeostasis in the gastrointestinal tract and suppressing the formation of colitis and colitis-associated adenocarcinoma formation. Furthermore, the study surprisingly reveals that the simple perturbation of the epithelial permeability barrier suffices to rapidly and efficiently induce malignant transformation of colonic epithelium.

## Materials and Methods

### Animal experiments

All procedures involving live animals were performed in an Association for Assessment and Accreditation of Laboratory Animals Care International-accredited vivarium following institutional guidelines and standard operating procedures. Within the study period, sentinels within the mouse holding room sporadically tested positive for helicobacter, murine norovirus, and mouse parvovirus, and tested negative for ectromelia virus, mouse rotavirus, Theiler's encephalomyelitis virus (GDVII strain), lymphocytic choriomeningitis virus, mycobacteria, mouse hepatitis virus, minute virus of mice, mouse polyoma virus, pneumonia virus of mice, reovirus type 3, Sendai virus, and fecal endo and ectoparasites. The NIDCR Institutional Animal Care and Use Committee approved the study. All studies were strictly littermate controlled. *St14* knock out (*St14*<sup>-/-</sup>) and conditional knockout (*St14*<sup>LoxP/LoxP</sup>) mice have been described previously (List *et al.*, 2002, List *et al.*, 2009). *Villin-Cre*<sup>+0</sup> [B6.SJL-Tg(Vil-Cre)997Gum/J] mice (Madison *et al.*, 2002) were purchased from The Jackson Laboratory (Bar Harbor, ME). All experimental animals were in a mixed 129/C57BL6/J/NIH Black Swiss/FVB/NJ background. The genotypes of all mice were determined by PCR of ear or tail biopsy DNA. *St14*<sup>+</sup> and *St14*<sup>LoxP</sup> alleles were detected using the primers 5'-CAGTGCTGTTTCAGCTTCCTCTT-3' and 5'-GTGGAGGTGGAGTTCTCATACG-5'. The presence of the *St14* knock out allele was

detected using primers 5'-GTGGAGGTGGAGTTCTCATACG-3' and 5'-GTGCGAGGCCAGAGGCCACTTGTGTAGCG-3'. The Cre transgene was detected using the primers 5'-GCATAACCAGTGAAACAGCATTGCTG-3' and 5'-GGACATGTTTCAGGGATCGCCAGGCG-3'. For antibiotics treatment, mice were given a combination of ampicillin (1 g/l, Sigma-Aldrich, St. Louis, MO), neomycin (1 g/l, Sigma-Aldrich), metronidazole (1 g/l, Sigma-Aldrich), and vancomycin (0.5 g/l, Sigma-Aldrich) in the drinking water for two weeks, starting immediately after weaning (P20).

### Quantitative PCR analysis

RNA was prepared from mouse organs by extraction in TRIzol reagent (Invitrogen, Carlsbad, CA), as recommended by the manufacturer. First strand cDNA synthesis was performed using oligo (dT) primers with the iScript™ cDNA synthesis kit (Bio-Rad Laboratories, Hercules, CA). An iCycler, gene expression analysis software, and IQ SYBR Green Supermix (all from Bio-Rad Laboratories) were used for quantitative PCR analysis in accordance with the manufacturer's instructions, using a primer complementary to sequence of matriptase exon 1, 5'-AACCATGGGTAGCAATCGGGGC-3', and matriptase exon 2, 5'-AACTCCACACCCTCCTCAAAGC-3' (annealing temperature 60 °C, denaturation temperature 95 °C, 40 cycles). Matriptase expression levels were normalized to glyceraldehyde-3-phosphate dehydrogenase (*Gapdh*) levels in each sample. *Gapdh* mRNA was amplified with the primers 5'-GTGAAGCAGGCATCTGAGG-3' and 5'-CATCGAAGGTGGAAGAGTGG-3' (annealing temperature 60 °C, denaturation temperature 95 °C, 40 cycles).

### Quantification of bacterial intestinal colonization

Bacterial DNA was isolated from feces using QIAamp DNA Stool Mini Kit (Qiagen, Valencia, CA) according to manufacturer's instructions. Bacterial DNA was quantified by qPCR analysis of bacterial 16S ribosomal DNA, amplified by primers: 8FM (5'-AGAGTTTGATCMTGGCTCAG-3') and Bact 5 15 R (5'-TTACCGCGGCKGCTGGCAC-3'). An iCycler, gene expression analysis software, and IQ SYBR Green Supermix were used for real-time PCR in accordance with the manufacturer's instructions. The thermal cycling program consisted of 95 °C for 10 min, followed by 40 cycles of 95 °C for 30 s, 55 °C for 30 s, 60 °C for 45 s, 65 °C for 15 s and 72 °C for 15 s. Helicobacter testing was performed as described previously (Feng *et al.*, 2005, Riley *et al.*, 1996).

### Intestinal tight junction assay

Fifty ul of 10 mg/ml EZ-Link Sulfo-NHSLC-Biotin (Thermo Fisher Scientific, Waltham, MA) in PBS containing 1 mmol/L CaCl<sub>2</sub> was injected into the lumen of distal colon and jejunum of three week old *St14*<sup>-</sup> and *St14*<sup>+</sup> littermates that were anesthetized by intraperitoneal injection of an anesthetic combination (ketamine [20 mg/ml], xylazine [2 mg/ml], 50 ul/10 g). After 3 min incubation, the mice were euthanized, and the injected portion of the intestine was excised and fixed in 10% neutral-buffered zinc formalin (Z-fix, Anatech, Battle Creek, MI) for 3 h, processed into paraffin and sectioned. Five μm sections were blocked for 30 min in blocking solution (5% bovine serum albumin in PBS), and then

incubated for 1 h at room temperature with streptavidin Alexa Fluor 448 conjugate (Invitrogen) (5 ug/ml) in blocking solution. Sections were washed three times with PBS and mounted with VECTASHIELD HardSet Mounting Medium with DAPI (Vector Laboratories, Burlingame, CA). Images were acquired on an Axio Imager. Z1 microscope using an AxioCam HRc/MRm digital camera (Carl Zeiss Ltd, Jena, Germany).

### Histopathology

Mice were euthanized by CO<sub>2</sub> inhalation. Tissues were fixed for 24 h in Z-fix, processed into paraffin, cut into 5 µm sections, and stained with hematoxylin and eosin (H&E). For visualization of mucin production, sections were stained with the Periodic Acid-Schiff (PAS) kit (Sigma-Aldrich) or Alcian Blue (1% Alcian Blue in 3% acetic acid). Collagen was detected using Masson-trichrome staining.

### Immunohistochemistry

Tissue sections were prepared and antigens were retrieved by heating in epitope retrieval buffer (0.01 M sodium citrate, pH 6.5) or Epitop Retrieval Buffer-Reduced pH (Bethyl Laboratories, Montgomery, TX) for matriptase IHC. The sections were blocked for 1 h in 5% bovine serum albumin (Sigma-Aldrich), or 10% horse serum (for matriptase IHC) in PBS, and incubated overnight at 4 C with primary antibody: matriptase (Sheep, Polyclonal, R&D Systems, Minneapolis, MN), cytokeratins (Rabbit, Polyclonal, DakoCytomation, Carpinteria, CA), LYVE-1 (Goat, Polyclonal, R&D Systems), β-catenin (Rabbit, Monoclonal, Cell Signaling, Danvers, MA), laminin (Rabbit, Polyclonal, Sigma-Aldrich), BrdU (Rat, Monoclonal, Accurate Chemicals & Scientific, Westbury, NY), CD3 (Rabbit, Polyclonal, DakoCytomation), κ-light chain (Rabbit, Polyclonal, DakoCytomation), Ki67 (Rabbit, Polyclonal, Novocastra, Westbury, NY), myeloperoxidase (Rabbit, Polyclonal, DakoCytomation), and Sox9 (Rabbit, Polyclonal, Millipore, Temecula, CA). Bound antibodies were visualized using either biotin-conjugated horse anti-goat, goat anti-rabbit, goat anti-rat (Vector Laboratories, Burlingame, CA), rabbit anti-sheep (Thermo Scientific, Rockford, IL), or alkaline phosphatase-conjugated donkey anti-rabbit (DakoCytomation) secondary antibodies and a VECTASTAIN ABC kit (Vector Laboratories) using 3,3'-diaminobenzidine substrate (Sigma-Aldrich) or Vulcan Fast Red Chromogen Kit 2 (Biocare Medical, Concord, CA). Hematoxylin was the counterstain.

### Immunoblotting

Approximately 1 cm of the distal part of large intestine was homogenized and lysed in 25 mM Tris-HCl, pH 7.6, 150 mM NaCl, 1% NP-40, 1% sodium deoxycholate, 0.1% SDS and protease inhibitor cocktail (Sigma). Boiled and reduced samples were subjected to immunoblotting using primary antibodies: anti-β-catenin (Rabbit, Monoclonal, Cell Signaling), anti-phospho-SMAD1/5 (Rabbit, monoclonal, Cell Signaling), anti-Notch1 (Rabbit, monoclonal, Cell Signaling), and anti-GAPDH (Rabbit, polyclonal, Santa Cruz, Santa Cruz, CA). The signal was detected with secondary anti-rabbit antibody conjugated to either alkaline phosphatase (Dako) or horseradish peroxidase (Thermo Scientific).

## Microarray analysis

Microarray analysis of gene expression was performed using Mouse GE 4×44K v2 Microarray slides (Agilent Technologies, Santa Clara, CA) according to manufacturer's instructions. Briefly, colon tissue was dissected from four pairs of *St14<sup>-</sup>* and littermate *St14<sup>+</sup>* mice. RNA was isolated using TRIzol reagent, as recommended by the manufacturer. The quality and the integrity of the RNA was determined by the 2100 Bioanalyzer platform (Agilent Technologies). Isolated colon RNA together with Universal Mouse Reference RNA (Agilent Technologies) was labeled using the Two-color Quick Amp Labeling Kit (Agilent Technologies). Labeled RNA was hybridized to the slides overnight. After washing the slides were scanned using a High Resolution Microarray Scanner. The raw microarray image files were read and processed with Feature Extraction Software. The analysis of microarray data was performed using Gene Spring Software (all from Agilent Technologies). Gene expression was normalized to the universal reference RNA. From the original data set, only probes flagged as detected at least in one sample were selected. These data sets were further filtered for probes with 2-or more fold change in expression between *St14<sup>+</sup>* and *St14<sup>-</sup>* tissue. Statistical analysis of these data sets led to the identification of probes with significantly different change in gene expression using unpaired Student's t-test with Benjamini-Hochberg multiple testing correction. Probes with  $P < 0.05$  were considered significant and are shown in Tables 2 and 3.

## Histomorphometric analysis

Five control *St14<sup>-</sup>* and six antibiotics treated *St14<sup>-</sup>* mice were analyzed. To determine the mucosal thickness, 2 mm of the distal colon mucosa adjacent to squamous epithelium of the rectum was identified on a H&E section and the area was calculated using Aperio ImageScope software (Aperio, Vista, CA). For the quantification of proliferation, differentiation and inflammatory infiltrates, seven individual areas of distal colon on each slide were selected for counting. The number of counts was normalized to the surface of the selected area and averaged for each individual animal.

## Supplementary Material

Refer to Web version on PubMed Central for supplementary material.

## Acknowledgments

We thank Drs. Jerrold M. Ward, Robert D. Cardiff, and Stephen M. Hewitt for pathology advice, Drs. Vyomesh Patel and Kantima Leelahavanichkul for help with the array analysis, Dr. Myrna Mandel for helicobacter testing, and Drs. Silvio Gutkind and Mary Jo Danton for critically reviewing this manuscript. Histology was performed by Histoserv, Inc., Germantown, MD. Supported by the NIDCR Intramural Research Program (T.H.B).

## References

- Acuff HB, Sinnamon M, Fingleton B, Boone B, Levy SE, Chen X, et al. Analysis of host- and tumor-derived proteinases using a custom dual species microarray reveals a protective role for stromal matrix metalloproteinase-12 in non-small cell lung cancer. *Cancer Res.* 2006; 66:7968–7975. [PubMed: 16912171]
- Andreasen PA, Egelund R, Petersen HH. The plasminogen activation system in tumor growth, invasion, and metastasis. *Cell Mol Life Sci.* 2000; 57:25–40. [PubMed: 10949579]

- Balbin M, Fueyo A, Tester AM, Pendas AM, Pitiot AS, Astudillo A, et al. Loss of collagenase-2 confers increased skin tumor susceptibility to male mice. *Nat Genet.* 2003; 35:252–257. [PubMed: 14517555]
- Berg DJ, Davidson N, Kuhn R, Muller W, Menon S, Holland G, et al. Enterocolitis and colon cancer in interleukin-10-deficient mice are associated with aberrant cytokine production and CD4(+) TH1-like responses. *J Clin Invest.* 1996; 98:1010–1020. [PubMed: 8770874]
- Bhatt AS, Welm A, Farady CJ, Vasquez M, Wilson K, Craik CS. Coordinate expression and functional profiling identify an extracellular proteolytic signaling pathway. *Proc Natl Acad Sci U S A.* 2007
- Borgono CA, Diamandis EP. The emerging roles of human tissue kallikreins in cancer. *Nat Rev Cancer.* 2004; 4:876–890. [PubMed: 15516960]
- Bugge TH, Antalis TM, Wu Q. Type II transmembrane serine proteases. *J Biol Chem.* 2009; 284:23177–23181. [PubMed: 19487698]
- Buzza MS, Netzel-Arnett S, Shea-Donohue T, Zhao A, Lin CY, List K, et al. Membrane-anchored serine protease matriptase regulates epithelial barrier formation and permeability in the intestine. *Proc Natl Acad Sci U S A.* 2010; 107:4200–4205. [PubMed: 20142489]
- Cheng H, Fukushima T, Takahashi N, Tanaka H, Kataoka H. Hepatocyte growth factor activator inhibitor type 1 regulates epithelial to mesenchymal transition through membrane-bound serine proteinases. *Cancer Res.* 2009; 69:1828–1835. [PubMed: 19223533]
- Danese S, Mantovani A. Inflammatory bowel disease and intestinal cancer: a paradigm of the Yin-Yang interplay between inflammation and cancer. *Oncogene.* 2010; 29:3313–3323. [PubMed: 20400974]
- de Lau W, Barker N, Clevers H. WNT signaling in the normal intestine and colorectal cancer. *Front Biosci.* 2007; 12:471–491. [PubMed: 17127311]
- Deng L, Zhou JF, Sellers RS, Li JF, Nguyen AV, Wang Y, et al. A novel mouse model of inflammatory bowel disease links mammalian target of rapamycin-dependent hyperproliferation of colonic epithelium to inflammation-associated tumorigenesis. *Am J Pathol.* 2010; 176:952–967. [PubMed: 20042677]
- Engle SJ, Ormsby I, Pawlowski S, Boivin GP, Croft J, Balish E, et al. Elimination of colon cancer in germ-free transforming growth factor beta 1-deficient mice. *Cancer Res.* 2002; 62:6362–6366. [PubMed: 12438215]
- Erdman SE, Poutahidis T, Tomczak M, Rogers AB, Cormier K, Plank B, et al. CD4+ CD25+ regulatory T lymphocytes inhibit microbially induced colon cancer in Rag2-deficient mice. *Am J Pathol.* 2003; 162:691–702. [PubMed: 12547727]
- Feng S, Ku K, Hodzic E, Lorenzana E, Freet K, Barthold SW. Differential detection of five mouse-infecting helicobacter species by multiplex PCR. *Clin Diagn Lab Immunol.* 2005; 12:531–536. [PubMed: 15817762]
- Forbs D, Thiel S, Stella MC, Sturzebecher A, Schweinitz A, Steinmetzer T, et al. In vitro inhibition of matriptase prevents invasive growth of cell lines of prostate and colon carcinoma. *Int J Oncol.* 2005; 27:1061–1070. [PubMed: 16142324]
- Garrett WS, Punit S, Gallini CA, Michaud M, Zhang D, Sigrist KS, et al. Colitis-associated colorectal cancer driven by T-bet deficiency in dendritic cells. *Cancer Cell.* 2009; 16:208–219. [PubMed: 19732721]
- Gaspar C, Cardoso J, Franken P, Molenaar L, Morreau H, Moslein G, et al. Cross-species comparison of human and mouse intestinal polyps reveals conserved mechanisms in adenomatous polyposis coli (APC)-driven tumorigenesis. *Am J Pathol.* 2008; 172:1363–1380. [PubMed: 18403596]
- Hale LP, Perera D, Gottfried MR, Maggio-Price L, Srinivasan S, Marchuk D. Neonatal co-infection with helicobacter species markedly accelerates the development of inflammation-associated colonic neoplasia in IL-10(–/–) mice. *Helicobacter.* 2007; 12:598–604. [PubMed: 18001399]
- Hardwick JC, Kodach LL, Offerhaus GJ, van den Brink GR. Bone morphogenetic protein signalling in colorectal cancer. *Nat Rev Cancer.* 2008; 8:806–812. [PubMed: 18756288]
- Ihara S, Miyoshi E, Ko JH, Murata K, Nakahara S, Honke K, et al. Prometastatic effect of N-acetylglucosaminyltransferase V is due to modification and stabilization of active matriptase by adding beta 1–6 GlcNAc branching. *J Biol Chem.* 2002; 277:16960–16967. [PubMed: 11864986]

- Jin X, Yagi M, Akiyama N, Hirosaki T, Higashi S, Lin CY, et al. Matriptase activates stromelysin (MMP-3) and promotes tumor growth and angiogenesis. *Cancer Sci.* 2006; 97:1327–1334. [PubMed: 16999819]
- Kaiser S, Park YK, Franklin JL, Halberg RB, Yu M, Jessen WJ, et al. Transcriptional recapitulation and subversion of embryonic colon development by mouse colon tumor models and human colon cancer. *Genome Biol.* 2007; 8:R131. [PubMed: 17615082]
- Kaser A, Zeissig S, Blumberg RS. Inflammatory bowel disease. *Annu Rev Immunol.* 2010; 28:573–621. [PubMed: 20192811]
- Kessenbrock K, Plaks V, Werb Z. Matrix metalloproteinases: regulators of the tumor microenvironment. *Cell.* 2010; 141:52–67. [PubMed: 20371345]
- Kilpatrick LM, Harris RL, Owen KA, Bass R, Ghorayeb C, Bar-Or A, et al. Initiation of plasminogen activation on the surface of monocytes expressing the type II transmembrane serine protease matriptase. *Blood.* 2006; 108:2616–2623. [PubMed: 16794252]
- Kim MG, Chen C, Lyu MS, Cho EG, Park D, Kozak C, et al. Cloning and chromosomal mapping of a gene isolated from thymic stromal cells encoding a new mouse type II membrane serine protease, epithin, containing four LDL receptor modules and two CUB domains. *Immunogenetics.* 1999; 49:420–428. [PubMed: 10199918]
- Lacy-Hulbert A, Smith AM, Tissire H, Barry M, Crowley D, Bronson RT, et al. Ulcerative colitis and autoimmunity induced by loss of myeloid alpha<sub>v</sub> integrins. *Proc Natl Acad Sci U S A.* 2007; 104:15823–15828. [PubMed: 17895374]
- Lee SL, Dickson RB, Lin CY. Activation of hepatocyte growth factor and urokinase/plasminogen activator by matriptase, an epithelial membrane serine protease. *J Biol Chem.* 2000; 275:36720–36725. [PubMed: 10962009]
- Lin CY, Anders J, Johnson M, Sang QA, Dickson RB. Molecular cloning of cDNA for matriptase, a matrix-degrading serine protease with trypsin-like activity. *J Biol Chem.* 1999; 274:18231–18236. [PubMed: 10373424]
- List K, Haudenschild CC, Szabo R, Chen W, Wahl SM, Swaim W, et al. Matriptase/MT-SP1 is required for postnatal survival, epidermal barrier function, hair follicle development, and thymic homeostasis. *Oncogene.* 2002; 21:3765–3779. [PubMed: 12032844]
- List K, Szabo R, Molinolo A, Sriuranpong V, Redeye V, Murdock T, et al. Deregulated matriptase causes ras-independent multistage carcinogenesis and promotes ras-mediated malignant transformation. *Genes Dev.* 2005; 19:1934–1950. [PubMed: 16103220]
- List K, Kosa P, Szabo R, Bey AL, Wang CB, Molinolo A, et al. Epithelial integrity is maintained by a matriptase-dependent proteolytic pathway. *Am J Pathol.* 2009; 175:1453–1463. [PubMed: 19717635]
- Lopez-Otin C, Matrisian LM. Emerging roles of proteases in tumour suppression. *Nat Rev Cancer.* 2007; 7:800–808. [PubMed: 17851543]
- Lopez-Otin C, Palavalli LH, Samuels Y. Protective roles of matrix metalloproteinases: from mouse models to human cancer. *Cell Cycle.* 2009; 8:3657–3662. [PubMed: 19844170]
- Madison BB, Dunbar L, Qiao XT, Braunstein K, Braunstein E, Gumucio DL. Cis elements of the villin gene control expression in restricted domains of the vertical (crypt) and horizontal (duodenum, cecum) axes of the intestine. *J Biol Chem.* 2002; 277:33275–33283. [PubMed: 12065599]
- Maggio-Price L, Treuting P, Zeng W, Tsang M, Bielefeldt-Ohmann H, Iritani BM. Helicobacter infection is required for inflammation and colon cancer in SMAD3-deficient mice. *Cancer Res.* 2006; 66:828–838. [PubMed: 16424015]
- McCawley LJ, Crawford HC, King LE Jr, Mudgett J, Matrisian LM. A protective role for matrix metalloproteinase-3 in squamous cell carcinoma. *Cancer Res.* 2004; 64:6965–6972. [PubMed: 15466188]
- McCawley LJ, Wright J, LaFleur BJ, Crawford HC, Matrisian LM. Keratinocyte expression of MMP3 enhances differentiation and prevents tumor establishment. *Am J Pathol.* 2008; 173:1528–1539. [PubMed: 18832569]
- Medema JP, Vermeulen L. Microenvironmental regulation of stem cells in intestinal homeostasis and cancer. *Nature.* 2011; 474:318–326. [PubMed: 21677748]

- Mohamed MM, Sloane BF. Cysteine cathepsins: multifunctional enzymes in cancer. *Nat Rev Cancer*. 2006; 6:764–775. [PubMed: 16990854]
- Netzel-Arnett S, Hooper JD, Szabo R, Madison EL, Quigley JP, Bugge TH, et al. Membrane anchored serine proteases: a rapidly expanding group of cell surface proteolytic enzymes with potential roles in cancer. *Cancer Metastasis Rev*. 2003; 22:237–258. [PubMed: 12784999]
- Netzel-Arnett S, Currie BM, Szabo R, Lin CY, Chen LM, Chai KX, et al. Evidence for a matriptase-prostasin proteolytic cascade regulating terminal epidermal differentiation. *J Biol Chem*. 2006; 281:32941–32945. [PubMed: 16980306]
- Newman JV, Kosaka T, Sheppard BJ, Fox JG, Schauer DB. Bacterial infection promotes colon tumorigenesis in Apc(Min/+) mice. *J Infect Dis*. 2001; 184:227–230. [PubMed: 11424022]
- Oberst MD, Williams CA, Dickson RB, Johnson MD, Lin CY. The activation of matriptase requires its noncatalytic domains, serine protease domain, and its cognate inhibitor. *J Biol Chem*. 2003; 278:26773–26779. [PubMed: 12738778]
- Okayasu I, Ohkusa T, Kajiura K, Kanno J, Sakamoto S. Promotion of colorectal neoplasia in experimental murine ulcerative colitis. *Gut*. 1996; 39:87–92. [PubMed: 8881816]
- Okayasu I, Yamada M, Mikami T, Yoshida T, Kanno J, Ohkusa T. Dysplasia and carcinoma development in a repeated dextran sulfate sodium-induced colitis model. *J Gastroenterol Hepatol*. 2002; 17:1078–1083. [PubMed: 12201867]
- Owen KA, Qiu D, Alves J, Schumacher AM, Kilpatrick LM, Li J, et al. Pericellular activation of hepatocyte growth factor by the transmembrane serine proteases matriptase and hepsin, but not by the membrane-associated protease uPA. *Biochem J*. 2010; 426:219–228. [PubMed: 20015050]
- Palavalli LH, Prickett TD, Wunderlich JR, Wei X, Burrell AS, Porter-Gill P, et al. Analysis of the matrix metalloproteinase family reveals that MMP8 is often mutated in melanoma. *Nat Genet*. 2009; 41:518–520. [PubMed: 19330028]
- Rakoff-Nahoum S, Paglino J, Eslami-Varzaneh F, Edberg S, Medzhitov R. Recognition of commensal microflora by toll-like receptors is required for intestinal homeostasis. *Cell*. 2004; 118:229–241. [PubMed: 15260992]
- Reinheckel T, Hagemann S, Dollwet-Mack S, Martinez E, Lohmuller T, Zlatkovic G, et al. The lysosomal cysteine protease cathepsin L regulates keratinocyte proliferation by control of growth factor recycling. *J Cell Sci*. 2005; 118:3387–3395. [PubMed: 16079282]
- Rhodes DR, Yu J, Shanker K, Deshpande N, Varambally R, Ghosh D, et al. ONCOMINE: a cancer microarray database and integrated data-mining platform. *Neoplasia*. 2004; 6:1–6. [PubMed: 15068665]
- Riley LK, Franklin CL, Hook RR Jr, Besch-Williford C. Identification of murine helicobacters by PCR and restriction enzyme analyses. *J Clin Microbiol*. 1996; 34:942–946. [PubMed: 8815113]
- Rudolph U, Finegold MJ, Rich SS, Harriman GR, Srinivasan Y, Brabet P, et al. Ulcerative colitis and adenocarcinoma of the colon in G alpha i2-deficient mice. *Nat Genet*. 1995; 10:143–150. [PubMed: 7663509]
- Saleh M, Trinchieri G. Innate immune mechanisms of colitis and colitis-associated colorectal cancer. *Nat Rev Immunol*. 2011; 11:9–20. [PubMed: 21151034]
- Sales KU, Masedunskas A, Bey AL, Rasmussen AL, Weigert R, List K, et al. Matriptase initiates activation of epidermal pro-kallikrein and disease onset in a mouse model of Netherton syndrome. *Nat Genet*. 2010; 42:676–683. [PubMed: 20657595]
- Sandilands A, Sutherland C, Irvine AD, McLean WH. Filaggrin in the frontline: role in skin barrier function and disease. *J Cell Sci*. 2009; 122:1285–1294. [PubMed: 19386895]
- Schreiber S, Rosenstiel P, Albrecht M, Hampe J, Krawczak M. Genetics of Crohn disease, an archetypal inflammatory barrier disease. *Nat Rev Genet*. 2005; 6:376–388. [PubMed: 15861209]
- Shah SA, Simpson SJ, Brown LF, Comiskey M, de Jong YP, Allen D, et al. Development of colonic adenocarcinomas in a mouse model of ulcerative colitis. *Inflamm Bowel Dis*. 1998; 4:196–202. [PubMed: 9741021]
- Smith FJ, Irvine AD, Terron-Kwiatkowski A, Sandilands A, Campbell LE, Zhao Y, et al. Loss-of-function mutations in the gene encoding filaggrin cause ichthyosis vulgaris. *Nat Genet*. 2006; 38:337–342. [PubMed: 16444271]

- Sternlicht MD, Lochter A, Sympon CJ, Huey B, Rougier JP, Gray JW, et al. The stromal proteinase MMP3/stromelysin-1 promotes mammary carcinogenesis. *Cell*. 1999; 98:137–146. [PubMed: 10428026]
- Sternlicht MD, Bissell MJ, Werb Z. The matrix metalloproteinase stromelysin-1 acts as a natural mammary tumor promoter. *Oncogene*. 2000; 19:1102–1113. [PubMed: 10713697]
- Su L, Shen L, Clayburgh DR, Nalle SC, Sullivan EA, Meddings JB, et al. Targeted epithelial tight junction dysfunction causes immune activation and contributes to development of experimental colitis. *Gastroenterology*. 2009; 136:551–563. [PubMed: 19027740]
- Suzuki M, Kobayashi H, Kanayama N, Saga Y, Lin CY, Dickson RB, et al. Inhibition of tumor invasion by genomic down-regulation of matriptase through suppression of activation of receptor-bound pro-urokinase. *J Biol Chem*. 2004; 279:14899–14908. [PubMed: 14747469]
- Szabo R, Bugge TH. Membrane anchored serine proteases in cell and developmental biology. *Annu Rev Cell and Developmental Biology*. 2011 In press.
- Szabo R, Rasmussen AL, Moyer AB, Kosa P, Schafer J, Molinolo A, et al. c-Met-induced epithelial carcinogenesis is initiated by the serine protease matriptase. *Oncogene*. 2011; 30:2003–2016. [PubMed: 21217780]
- Takeuchi T, Shuman MA, Craik CS. Reverse biochemistry: use of macromolecular protease inhibitors to dissect complex biological processes and identify a membrane-type serine protease in epithelial cancer and normal tissue. *Proc Natl Acad Sci U S A*. 1999; 96:11054–11061. [PubMed: 10500122]
- Takeuchi T, Harris JL, Huang W, Yan KW, Coughlin SR, Craik CS. Cellular localization of membrane-type serine protease 1 and identification of protease-activated receptor-2 and single-chain urokinase-type plasminogen activator as substrates. *J Biol Chem*. 2000; 275:26333–26342. [PubMed: 10831593]
- Tanimoto H, Underwood LJ, Wang Y, Shigemasa K, Parmley TH, O'Brien TJ. Ovarian tumor cells express a transmembrane serine protease: a potential candidate for early diagnosis and therapeutic intervention. *Tumour Biol*. 2001; 22:104–114. [PubMed: 11125283]
- Ustach CV, Huang W, Conley-LaComb MK, Lin CY, Che M, Abrams J, et al. A novel signaling axis of matriptase/PDGF-D/ss-PDGFR in human prostate cancer. *Cancer Res*. 2010; 70:9631–9640. [PubMed: 21098708]
- Van Limbergen J, Wilson DC, Satsangi J. The genetics of Crohn's disease. *Annu Rev Genomics Hum Genet*. 2009; 10:89–116. [PubMed: 19453248]
- Velcich A, Yang W, Heyer J, Fragale A, Nicholas C, Viani S, et al. Colorectal cancer in mice genetically deficient in the mucin Muc2. *Science*. 2002; 295:1726–1729. [PubMed: 11872843]
- Xavier RJ, Podolsky DK. Unravelling the pathogenesis of inflammatory bowel disease. *Nature*. 2007; 448:427–434. [PubMed: 17653185]
- Zeki SS, Graham TA, Wright NA. Stem cells and their implications for colorectal cancer. *Nat Rev Gastroenterol Hepatol*. 2011; 8:90–100. [PubMed: 21293509]
- Zhang Y, Cai X, Schlegelberger B, Zheng S. Assignment of human putative tumor suppressor genes ST13 (alias SNC6) and ST14 (alias SNC19) to human chromosome bands 22q13 and 11q24-->q25 by in situ hybridization. *Cytogenet Cell Genet*. 1998; 83:56–57. [PubMed: 9925927]

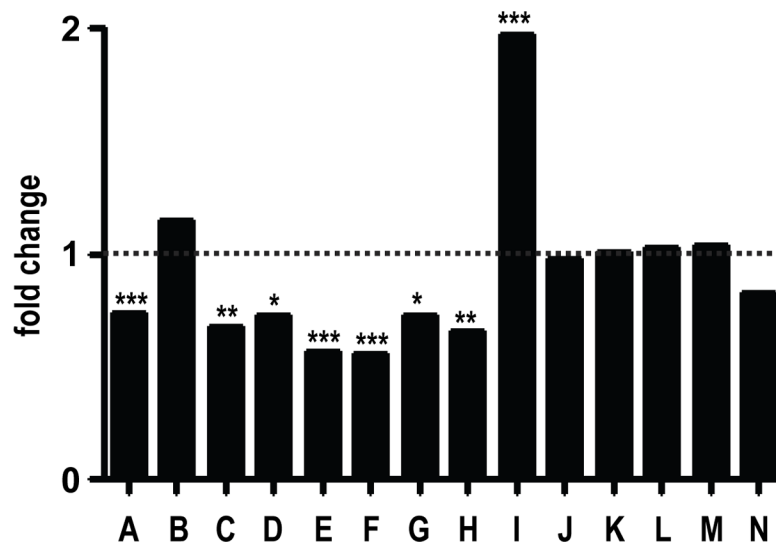


**Figure 1. Matriptase expression is downregulated in human colon adenomas and adenocarcinomas**

Expression of *ST14*, encoding matriptase, in 14 gene expression array studies of human colon adenomas and adenocarcinomas. Data are expressed as fold change relative to corresponding normal tissue. \* $P < 0.05$ , \*\* $P < 0.01$ , \*\*\* $P < 0.001$ . See Supplementary Table 1 for details and references.

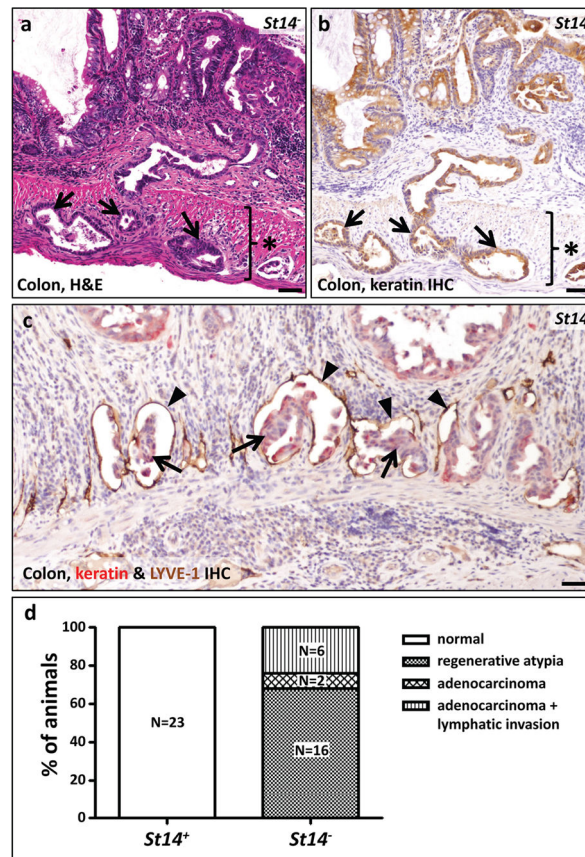


**Figure 2. Rapid and spontaneous malignant transformation of *St14*-ablated colonic epithelium**  
**(a)** Representative example of adenocarcinoma in the large intestine of an eight week old *St14*<sup>-</sup> mouse. Tumor cells invading the muscularis externa (**star**) are shown with **arrows**.  
**(b)** The epithelial origin of the tumor cells invading the muscularis externa (**star**) is demonstrated by immunohistochemical staining for keratin (examples with **arrows**). **(c)** Combined immunohistochemical staining for keratin in red (examples with **arrows**) and the lymphatic vessel marker LYVE-1 in brown (examples with **arrowheads**) shows invasion of malignant cells into lymphatic vessels of a seven week old *St14*<sup>-</sup> mouse. Scale bar for **a**, **b**, and **c** = 100  $\mu$ m. **(d)** Enumeration of colonic lesions in four to 18 week old *St14*<sup>+</sup> (left) and littermate *St14*<sup>-</sup> mice (right), showing adenocarcinoma with lymphatic invasion in 6, adenocarcinoma without lymphatic invasion in 2, and regenerative atypia in the remaining 16 *St14*<sup>-</sup> mice. See Table 1 for additional details.

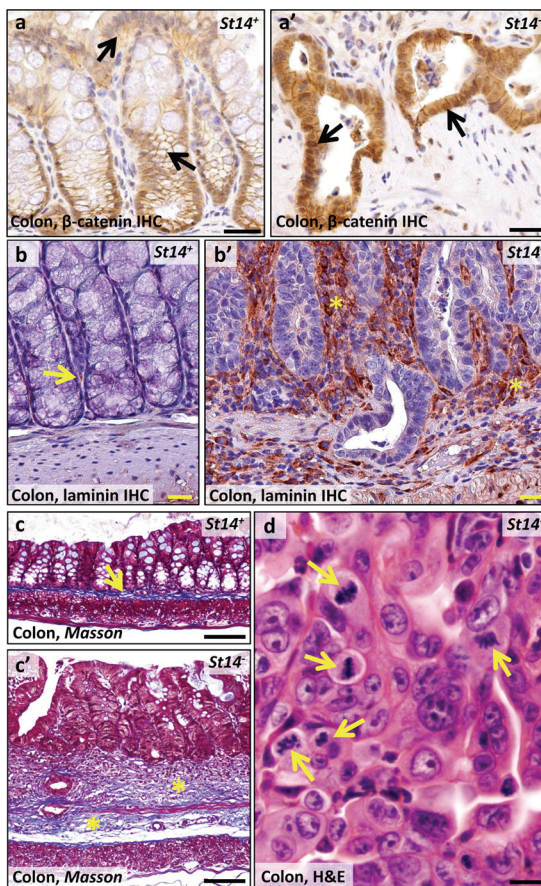


**Figure 3. Characterization of matriptase ablation-associated colon adenocarcinoma** (a,a') Immunohistochemical staining of eight week old *St14*<sup>+</sup> (a) and littermate *St14*<sup>-</sup> (a') colons for  $\beta$ -catenin shows a membrane-associated  $\beta$ -catenin localization in *St14*<sup>+</sup> epithelial cells (arrows in a), as compared to cytoplasmic and nuclear localization in adenocarcinomas of *St14*<sup>-</sup> colons (examples with arrows in a'). (b,b') Immunohistochemical staining for the basement membrane marker laminin in 15 week old *St14*<sup>+</sup> (b) and littermate *St14*<sup>-</sup> (b') mice shows the normal appearance of the basement membrane (example with arrow in b) in *St14*<sup>+</sup> mice. Loss of matriptase expression leads to increased deposition of laminin (examples with stars in b') and loss of normal structure of the basement membrane. (c,c') Masson Trichrome staining of the colon of six week old *St14*<sup>+</sup> (c) and littermate *St14*<sup>-</sup> (c') mice shows connective tissue in the submucosa of a normal colon (example with arrow in c) and fibrosis of both the mucosa and submucosa of *St14*<sup>-</sup> colon (examples with stars in c'). (d) High magnification shows the cytological appearance of adenocarcinomas of *St14*<sup>-</sup> mice. Atypical mitosis is shown by arrows. Scale bar = 200  $\mu$ m (a, a',b,b',c,c') and 20  $\mu$ m (d).

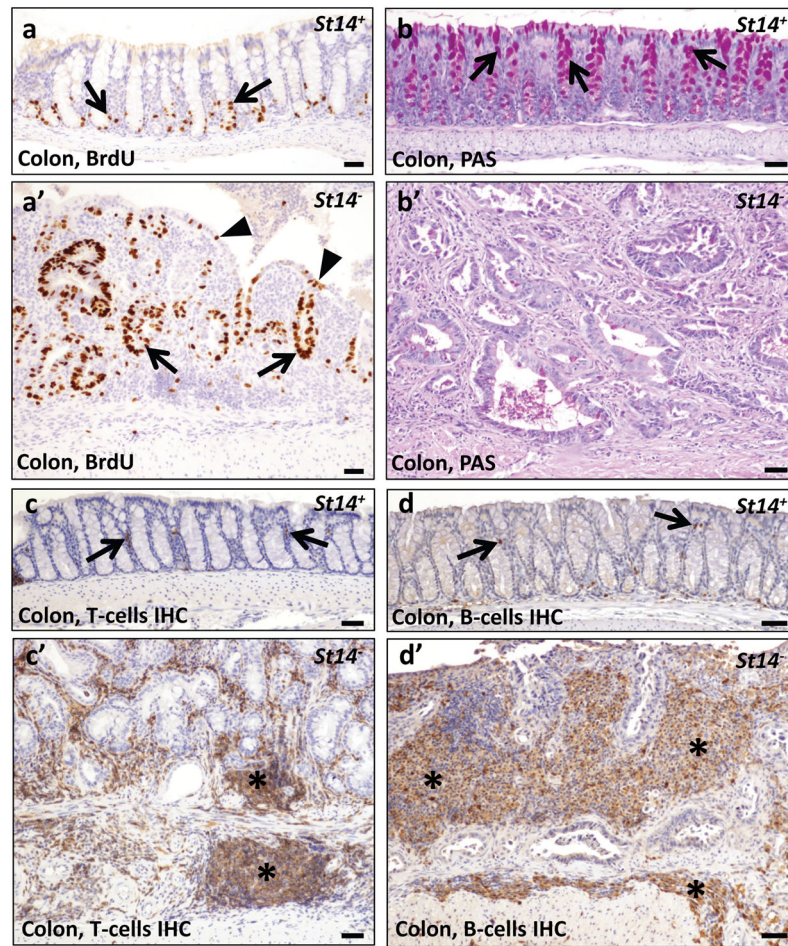


**Figure 4. Characterization of matriptase ablation-associated colon adenocarcinoma** (a,a') BrdU staining of eight week old *St14*<sup>+</sup> (a) and littermate *St14*<sup>-</sup> (a') mice shows proliferation restricted to the bottom of the crypts of normal colons (examples with **arrows** in a). In *St14*<sup>-</sup> colon, proliferating cells are found both in the bottom (examples with **arrows** in a') and distal parts of crypts (examples with **arrowheads** in a'). (b,b') Periodic Acid-Schiff (PAS) staining of mucopolysaccharides produced by differentiated goblet cells in the colon of eleven week old *St14*<sup>+</sup> (b) and littermate *St14*<sup>-</sup> (b') mice. Red staining shows mucin in the normal colon (**arrows** in b). Absence of red staining in (b') indicates cessation of mucin production in matriptase-ablated colon. (c,c',d,d') Immunohistochemical staining for T-cells (c,c') and B-cells (d,d') in, respectively, seven and 15 week old *St14*<sup>+</sup> (c, d) and littermate *St14*<sup>-</sup> (c',d') colons. Baseline levels of T- and B-cells in the lamina propria of *St14*<sup>+</sup> colon (examples with **arrows** in d and c) and abundance of T- and B-cells in both mucosa and submucosa of *St14*<sup>-</sup> colons (examples with **stars** in c',d'). Scale bar = 100  $\mu$ m.

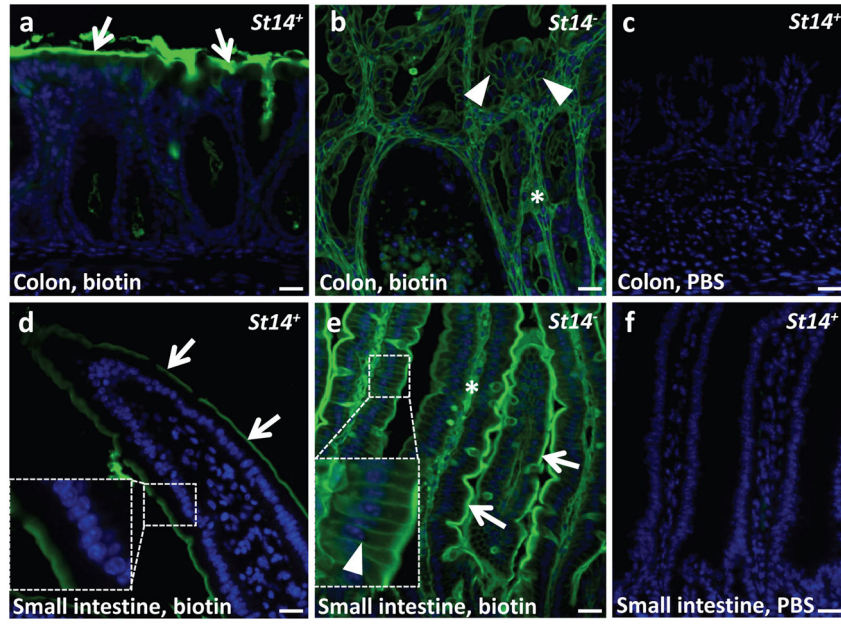


**Figure 5. Matriptase-ablated colon is leaky**

The lumen of the colon and small intestine of weaning age *St14*<sup>+</sup> and littermate *St14*<sup>-</sup> animals was injected with Sulfo-NHS-LC-Biotin in PBS (**a,b,d,e**) or PBS (**c,f**). After three min, the intestine was excised, sectioned, and stained for biotin (**green**). Nuclei were stained with 4,6-diamino-2-phenylindol (**blue**). **Arrows** in **a**, **d**, and **e** show biotin bound to the surface of the mucosa. **Arrowheads** in **b** and the **inset** in **e** show biotin labeling of the basolateral membrane of polarized epithelial cells. The diffusion of biotin into intercellular space was not observed in the normal colon or small intestine (**a,d**, also compare **insets** in **d** and **e**). Stars show biotin labeling of connective tissue of both matriptase-ablated colon (**b**) and small intestine (**e**). There was no signal for biotin in colon and small intestine (**c,f**) injected with PBS. Scale bar = 20  $\mu$ m.

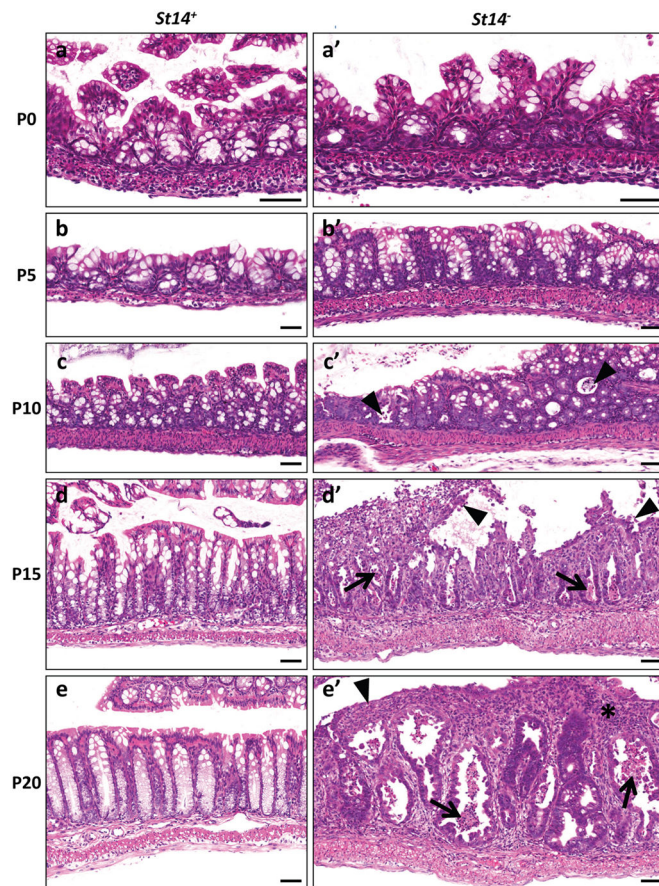


**Figure 6. Progressive postnatal loss of epithelial integrity of matriptase-ablated colon precedes malignant transformation**

Histological appearance of *St14*<sup>+</sup> (**a–e**) and littermate *St14*<sup>–</sup> (**a'–e'**) colons at postnatal day 0 (**a,a'**), 5 (**b,b'**), 10 (**c,c'**), 15 (**d,d'**), and 20 (**e,e'**). No histological differences can be observed between normal and matriptase-ablated colon at days 0 and 5 (compare **a** and **a'**, **b** and **b'**). At day 10, *St14*<sup>–</sup> colons show sporadic foci of detaching and apoptotic cells (**arrowheads** in **c'**). This phenotype is significantly stronger at days 15 and 20 with extensive anoikis (**arrowheads** in **d'**), apoptotic cells (**arrows** in **d', e'**), ulcerations (**arrowhead** in **e'**) and inflammatory cell infiltrates (**star** in **e'**). Scale bar = 100  $\mu$ m.

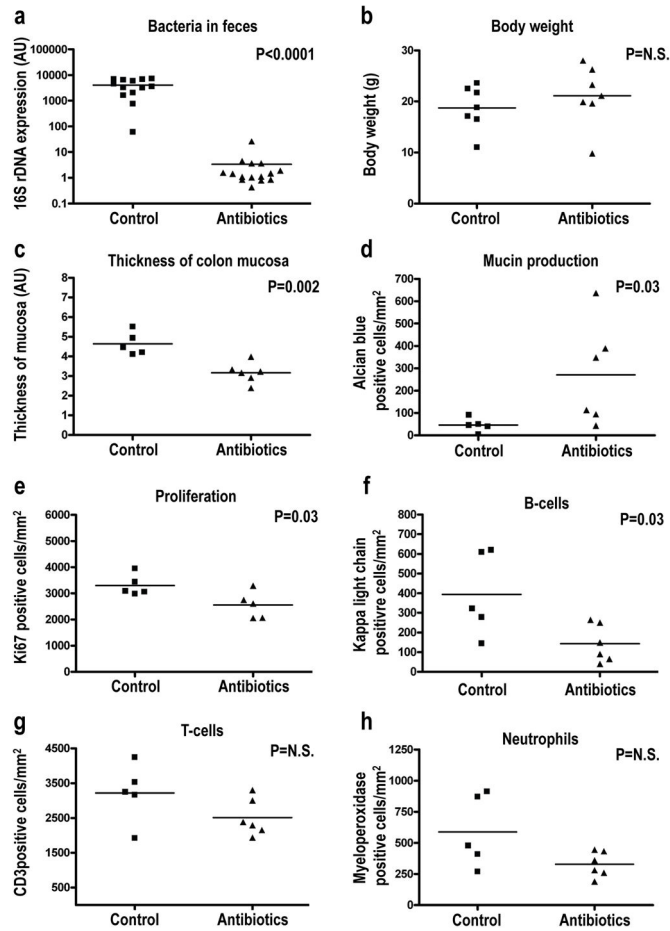


**Figure 7. The resident microbiota contributes to preneoplastic progression of matriptase-ablated colon**

Littermate *St14*<sup>-</sup> mice were kept on regular water (**control** in **a–h**) or treated with a combination of ampicillin, neomycin, metronidazole, and vancomycin in the drinking water (**antibiotics** in **a–h**) for two weeks starting immediately after weaning. The animals were euthanized, the feces was used for the isolation of bacterial DNA, and the colonic tissue was subjected to quantitative histomorphometric analysis. **(a)** PCR quantification of 16S bacterial ribosomal DNA shows a 1 500-fold decrease in the intestinal microbiota of antibiotics treated (N=15) compared to control (N=13) mice. **(b)** Body weight of antibiotics treated (N=7) and control (N=7) is similar. **(c)** Decreased thickness of the mucosa of antibiotics treated (N=6) compared to control (N=5) mice. **(d–f)** Preservation of mucin production **(d)**, decreased proliferation **(e)**, and decreased infiltration of B-cells **(f)**, T-cells **(g)** and neutrophils **(h)** in antibiotics treated (N=6) compared to (N=5) mice. Statistical significance was calculated by Student's t-test (two-tailed) **(a–c, e–h)**, and non-parametric Mann-Whitney U-test (two-tailed) **(d)**, N.S. = not significant.

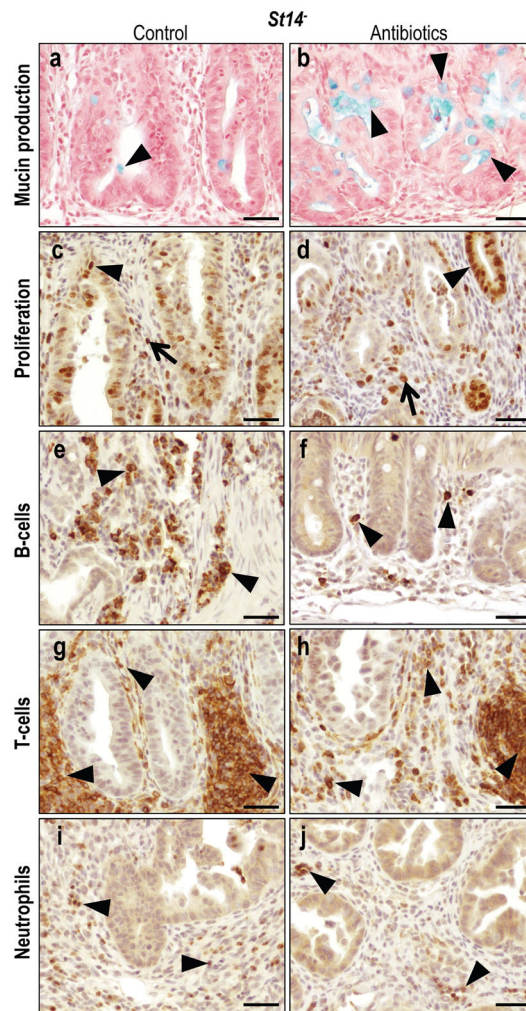


**Figure 8. Histological appearance of antibiotics treated matriptase-ablated colon** (a,b) Alcian Blue staining of mucin produced by differentiated goblet cells in untreated (a) and antibiotics treated (b) *St14*<sup>-</sup> colons. **Arrowheads** point to mucin (blue). (c,d) Immunohistochemical staining for Ki67 in untreated (c) and antibiotics treated (d) *St14*<sup>-</sup> mice show significantly decreased rates of proliferation of both epithelial cells (**arrowheads** in c,d) and connective tissue cells (**arrows** in c,d). (e-j) Immunohistochemical staining for B-cells (e,f), T-cells (g,h), and neutrophils (i,j) in untreated (e,g,i) and antibiotics treated (f,h,j) *St14*<sup>-</sup> colons shows reduced chronic (examples with **arrowheads** in e-h) and acute (examples with **arrowheads** in i and j) inflammatory cell infiltration. Scale bar = 50  $\mu$ m.

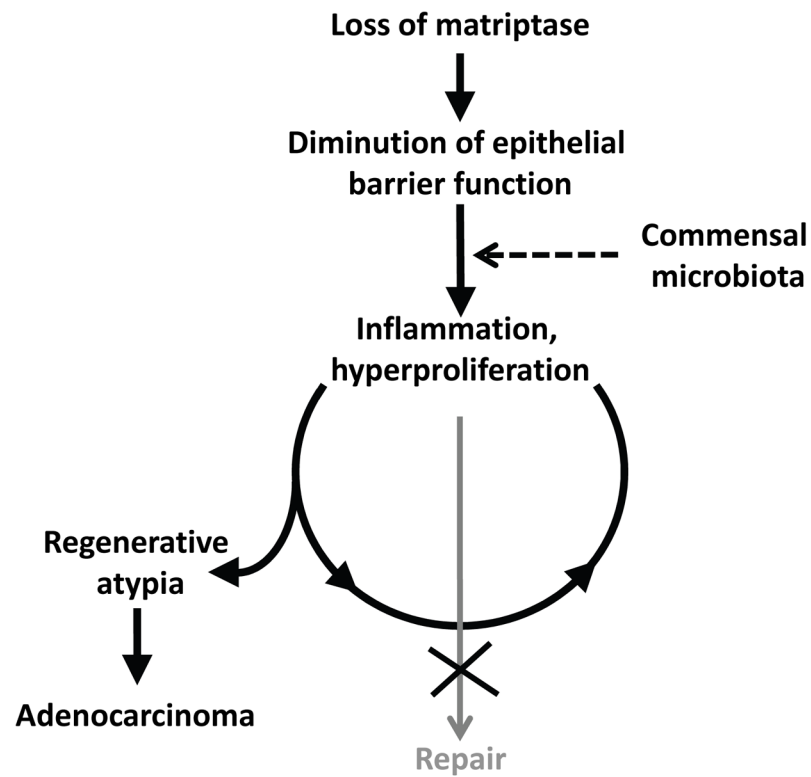


**Figure 9. Model for matriptase ablation-induced colon carcinogenesis**

Loss of matriptase from intestinal epithelium compromises epithelial barrier function thereby causing exposure of the commensal microbiota to resident immune cells. This triggers a repair response that includes activation of local inflammatory circuits and colonic stem cell activation. This response is perpetual, rather than transient, due to the intrinsic inability of matriptase-ablated to form a functional barrier. Persistent hyperproliferation of colonic stem cells within a DNA damaging chronic inflammatory microenvironment causes the formation of adenocarcinoma.

**Table 1**Intestinal lesions in *St14*<sup>-</sup> mice

Mouse	Gender	Age (days)	Diagnosis of intestinal lesions	Lymphatic invasion
MCV41	Male	31	Regenerative atypia	No
MCV52	Male	33	Adenocarcinoma	Yes
MCV55	Female	55	Regenerative atypia	No
MCV56	Female	55	Regenerative atypia	No
MCV59	Male	25	Regenerative atypia	No
MCV66	Male	28	Regenerative atypia	No
MCV70	Female	24	Regenerative atypia	No
MCV76	Male	129	Regenerative atypia	No
MCV127	Male	111	Regenerative atypia	No
MCV153	Male	79	Adenocarcinoma	No
MCV159	Female	26	Regenerative atypia	No
MCV162	Male	105	Adenocarcinoma	Yes
MCV173	Male	44	Regenerative atypia	No
MCV180	Female	131	Adenocarcinoma	No
MCV192	Male	44	Regenerative atypia	No
MCV204	Male	48	Adenocarcinoma	Yes
MCV234	Male	50	Adenocarcinoma	Yes
MCV256	Male	56	Adenocarcinoma	Yes
MCV359	Female	51	Adenocarcinoma	Yes
MCV366	Male	36	Regenerative atypia	No
MCV397	Male	39	Regenerative atypia	No
MCV461	Female	30	Regenerative atypia	No
MCV468	Male	22	Regenerative atypia	No
MCV1250	Male	67	Regenerative atypia	No

Table 2

Genes differentially regulated in 5 days old *St14*<sup>-</sup> mice

Agilent Probe ID	GenBank	Regulation	Fold change <sup>d</sup>	P-value <sup>e2</sup>	Gene symbol	Gene Name
A_51_P124665	NM_011474	up	17.86	0.001	<i>Spr2h</i>	small proline-rich protein 2H
A_51_P272066	NM_025929	up	9.40	0.001		RIKEN cDNA 2010109103 gene
A_51_P451966	NM_001177524	up	5.39	0.035	<i>Gml</i>	GPI anchored molecule like protein
A_52_P151240	NM_001195732	up	4.34	0.024	<i>Fam150a</i>	predicted gene, family with sequence similarity 150, member A
A_51_P243517	NM_010742	up	3.87	0.027	<i>Ly6d</i>	lymphocyte antigen 6 complex, locus D
A_51_P363187	NM_008176	up	3.13	0.001	<i>Cxcl1</i>	chemokine (C-X-C motif) ligand 1
A_51_P291950	NM_010266	up	2.91	0.037	<i>Gda</i>	guanine deaminase
A_52_P545650	NM_001174099	up	2.83	0.011	<i>Krt36</i>	keratin 36
A_51_P187121	NM_008127	up	2.63	0.028	<i>Gjib4</i>	gap junction protein, beta 4
A_51_P411495	XM_897643	up	2.50	0.045		RIKEN cDNA 4930465A12 gene
A_51_P420918	NM_020498	up	2.39	0.050	<i>Ly6i</i>	lymphocyte antigen 6 complex, locus I
A_51_P367880	NM_008474	up	2.35	0.037	<i>Krr84</i>	keratin 84
A_51_P120830	NM_019471	up	2.29	0.037	<i>Mmp10</i>	matrix metalloproteinase 10
A_51_P285639	NM_010291	up	2.28	0.011	<i>Gjib5</i>	gap junction protein, beta 5
A_51_P337308	NM_011315	up	2.27	0.019	<i>Saa3</i>	serum amyloid A 3
A_51_P228574	NM_146214	up	2.26	0.043	<i>Tat</i>	tyrosineaminotransferase
A_52_P562661	NM_010762	up	2.17	0.023	<i>Mal</i>	myelin and lymphocyte protein, T-cell differentiation protein
A_51_P499071	NM_010762	up	2.14	0.011	<i>Mal</i>	myelin and lymphocyte protein, T-cell differentiation protein
A_51_P503494	NM_018790	up	2.11	0.003	<i>Arc</i>	activity regulated cytoskeletal-associated protein
A_52_P299446	U90654	up	2.09	0.013		zinc-finger domain-containing protein
A_52_P220241	AK164337	up	2.09	0.032		RIKEN cDNA A430106P18 gene, hypothetical proline-rich region containing protein
A_51_P139678	NM_009264	up	2.09	0.021	<i>Spr1a</i>	small proline-rich protein 1A
A_51_P214275	NM_001174099	up	2.08	0.023	<i>Krt36</i>	keratin 36
A_51_P245090	NM_016689	up	2.07	0.020	<i>Aqp3</i>	aquaporin 3
A_51_P385099	NM_013693	up	2.06	0.019	<i>Tnf</i>	tumor necrosis factor
A_52_P26416	AF106279	up	2.05	0.045	<i>Lamc2</i>	laminin gamma2 chain
A_52_P445360	NM_023256	up	2.04	0.028	<i>Krr20</i>	keratin 20
A_51_P197528	NM_001099217	up	2.03	0.050	<i>Ly6c2</i>	lymphocyte antigen 6 complex, locus C2

Agilent Probe ID	GenBank	Regulation	Fold change <sup>1</sup>	P-value <sup>2</sup>	Gene symbol	Gene Name
A_52_P421234	NM_133832	up	2.02	0.011	<i>Rdh10</i>	retinol dehydrogenase 10
A_51_P323195	NM_172613	down	4.65	0.045	<i>Atp13a4</i>	ATPase type 13A4
A_52_P453814	NM_011242	down	3.09	0.045	<i>Rasgrp2</i>	RAS, guanyl releasing protein 2
A_51_P394847	NR_024599	down	2.86	0.045		predicted gene 11346
A_51_P492940	AK035376	down	2.63	0.045		RIKEN full-length enriched library, clone:9530027C22, unclassifiable product
A_51_P394172	NM_007954	down	2.44	0.021	<i>Esi1</i>	esterase 1
A_51_P375969	NM_053200	down	2.37	0.036	<i>Ces3</i>	carboxylesterase 3
A_52_P094399	NM_010039	down	2.34	0.048	<i>Defq4</i>	defensin, alpha, 4
A_52_P115950	AK036853	down	2.28	0.045		RIKEN full-length enriched library, clone:9930018I23, hypothetical protein
A_51_P391934	NM_029706	down	2.17	0.050	<i>Cpb1</i>	carboxypeptidase B1
A_51_P358037	NM_001014423	down	2.06	0.045	<i>Abi3bp</i>	ABI gene family, member 3 (NESH) binding protein
A_52_P819243	AK049777	down	2.05	0.045		RIKEN full-length enriched library, clone:C530048O03, hypothetical protein
A_51_P242967	NM_021308	down	2.01	0.011	<i>Piwil2</i>	piwi-like homolog 2

<sup>1</sup> Compared to expression in normal mucosa

<sup>2</sup> Student's t-test (two-tailed, unpaired, asymptotic), Benjamini-Hochberg multiple testing correction

Table 3

Genes differentially regulated in 10 days old *St14<sup>-</sup>* mice

Agilent Probe ID	GenBank	Regulation	Fold change <sup>1</sup>	P-value <sup>2</sup>	Gene symbol	Gene Name
A_52_P295432	NM_009141	up	32.09	0.044	<i>Cxcl5</i>	chemokine (C-X-C motif) ligand 5
A_51_P124665	NM_011474	up	28.95	0.037	<i>Sprr2h</i>	small proline-rich protein 2H
A_51_P256827	NM_013650	up	9.86	0.044	<i>SI00a8</i>	SI00 calcium binding protein A8 (calgranulin A)
A_51_P346938	NM_029796	up	8.30	0.044	<i>Lrg1</i>	leucine-rich alpha-2-glycoprotein 1
A_51_P363187	NM_008176	up	5.02	0.044	<i>Cxcl1</i>	chemokine (C-X-C motif) ligand 1
A_52_P487686	NM_001082546	up	4.36	0.044		cDNA sequence BC100530
A_51_P279437	NM_029662	up	3.98	0.048	<i>Mfsd2a</i>	major facilitator superfamily domain containing 2A
A_51_P359046	NM_020519	up	3.78	0.044	<i>Slurp1</i>	secreted Ly6/Plaur domain containing 1
A_51_P303160	NM_007482	up	3.71	0.044	<i>Arg1</i>	arginase
A_51_P451966	NM_001177524	up	3.58	0.044	<i>Gml</i>	GPI anchored molecule like protein
A_52_P1172382	Q8C9Z4 <sup>3</sup>	up	3.44	0.049		putative uncharacterized protein
A_52_P472324	NM_011414	up	3.13	0.044	<i>Slpi</i>	leukocyte peptidase inhibitor
A_51_P200544	NM_001001495	up	3.12	0.044	<i>Tnfr3</i>	TNFAIP3 interacting protein 3
A_51_P214275	NM_001174099	up	3.10	0.037	<i>Krt36</i>	keratin 36
A_51_P187461	NM_009044	up	3.03	0.044	<i>Rel</i>	reticuloendotheliosis oncogene
A_51_P116609	NM_025687	up	2.87	0.044	<i>Tex12</i>	testis expressed gene 12
A_52_P531140	NM_010416	up	2.81	0.044	<i>Hem1</i>	hematopoietic cell transcript 1
A_52_P545650	NM_001174099	up	2.74	0.038	<i>Krt36</i>	keratin 36
A_52_P31510	NM_008814	up	2.65	0.037	<i>Pdx1</i>	pancreatic and duodenal homeobox 1
A_52_P273394	AK137552	up	2.58	0.013	<i>Igl-5</i>	Immunoglobulin lambda chain 5
A_51_P272066	NM_025929	up	2.57	0.044		RIKEN cDNA 2010109103 gene
A_52_P116006	NM_010266	up	2.57	0.044	<i>Gda</i>	guanine deaminase
A_51_P225634	NM_027306	up	2.50	0.044	<i>Zdhhc25</i>	zinc finger, DHHC domain containing 25
A_52_P200286	NM_001167746	up	2.46	0.044	<i>Dnahc17</i>	dynein, axonemal, heavy chain 17
A_52_P482897	NM_009704	up	2.40	0.044	<i>Areg</i>	amphiregulin
A_52_P15388	NM_008522	up	2.33	0.044	<i>Lif</i>	lactotransferrin
A_51_P500082	NM_001110517	up	2.27	0.044		predicted gene 14446
A_52_P884135	AK085881	up	2.26	0.049		RIKEN full-length enriched library, clone:D830023G23, unclassifiable product

Agilent Probe ID	GenBank	Regulation	Fold change <sup>1</sup>	P-value <sup>2</sup>	Gene symbol	Gene Name
A_51_P165182	NM_028967	up	2.25	0.044	<b>Baf2</b>	basic leucine zipper transcription factor, ATP-like 2
A_52_P338066	NM_023137	up	2.24	0.049	<b>Ubd</b>	ubiquitin D
A_51_P454008	NM_008489	up	2.23	0.037	<b>Lbp</b>	lipopolysaccharide binding protein
A_51_P291950	NM_010266	up	2.22	0.044	<b>Gda</b>	guanine deaminase
A_52_P375047	NM_009184	up	2.22	0.039	<b>Ptk6</b>	PTK6 protein tyrosine kinase 6
A_51_P409349	NM_023655	up	2.21	0.046	<b>Trim29</b>	tripartite motif-containing 29
A_51_P228971	NM_023219	up	2.19	0.044	<b>Slc5a4b</b>	solute carrier family 5 (neutral amino acid transporters, system A), member 4b
A_51_P249989	NM_145133	up	2.19	0.047	<b>Tifa</b>	TRAF-interacting protein with forkhead-associated domain
A_52_P299446	U90654	up	2.18	0.044		zinc-finger domain-containing protein
A_52_P569327	AK045953	up	2.16	0.044	<b>Usp53</b>	mKIAA1350, ubiquitin specific peptidase 53
A_52_P208213	TC1638459	up	2.15	0.044		kalirin-12a, partial (6%)
A_51_P503494	NM_018790	up	2.08	0.049	<b>Arc</b>	activity regulated cytoskeletal-associated protein
A_52_P562661	NM_010762	up	2.06	0.044	<b>Mal</b>	myelin and lymphocyte protein, T-cell differentiation protein
A_51_P491987	NM_019955	up	2.04	0.044	<b>Ripk3</b>	receptor-interacting serine-threonine kinase 3
A_51_P499071	NM_010762	up	2.04	0.044	<b>Mal</b>	myelin and lymphocyte protein, T-cell differentiation protein
A_51_P181565	NM_010415	up	2.03	0.044	<b>Krt14</b>	keratin 14
A_51_P371500	BC049570	up	2.00	0.044	<b>Atp8b3</b>	heparin-binding EGF-like growth factor
A_51_P426055	AK048117	down	3.76	0.013		ATPase, class I, type 8B, member 3
A_52_P506984	ENSMUST00000044976 <sup>4</sup>	down	3.22	0.044	<b>Glyat</b>	RIKEN full-length enriched library, clone:C130035O18, unclassifiable product glycine-N-acyltransferase
A_52_P707475	AK053952	down	2.53	0.044		RIKEN full-length enriched library, clone:E230006P11, unclassifiable product
A_52_P739568	AK082480	down	2.17	0.044		RIKEN full-length enriched library, clone:C230053P15, unclassifiable product
A_52_P101443	NM_198111	down	2.14	0.044	<b>Akap6</b>	A kinase (PRKA) anchor protein 6

<sup>1</sup> Compared to expression in normal mucosa<sup>2</sup> Student's t-test (two-tailed, unpaired, asymptotic), Benjamini-Hochberg multiple testing correction<sup>3</sup> UniProtKB<sup>4</sup> Mouse Genome Informatics